phys. stat. sol. (a) **170**, 99 (1998)

Subject classification: 61.72.Mm; 68.35.Ct; S10.1

Atomic Structure of Symmetrical Tilt Grain Boundaries in Zinc Oxide with High Coincidence

W. WUNDERLICH[1])

Japan Fine Ceramics Center, 2-4-1 Mutsuno, Atsuta-ku, 456 Nagoya, Japan

(Received August 7, 1997; in revised form June 15, 1998)

Dedicated to Professor Dr. MANFRED RÜHLE on the occasion of his 60th birthday

The coincidence site lattice (CSL) theory is very successful in detecting grain boundaries with low energy and is applied to zinc oxide and aluminum nitride. Special symmetrical tilt ZnO-grain boundaries in *a*-axes orientation with low Σ values were selected for molecular dynamics simulations. The calculations lead to stable atomic structural units at the grain boundary core with 8 or 10 atoms, which have different bonding lengths than those in the single crystal and, hence, promise special electronic properties. The experimental HRTEM images show the well-defined atomic structure of CSL grain boundaries compared to others.

Die Koinzidenztheorie (CSL) ist sehr erfolgreich für die Bestimmung von Korngrenzen mit geringer Energie und wurde angewendet für Zinkoxid und Aluminiumnitrid. Spezielle, symmetrische ZnO-Kipp-Korngrenzen in *a*-Achsen-Orientierung mit niedrigen Σ-Werten wurden ausgewählt für molekulardynamische Simulationen. Die Rechnungen führen zu stabilen, strukturellen Einheiten im Kern der Korngrenze mit 8 oder 10 Atomen, die verglichen mit dem Einkristall verschiedene Bindungslängen aufweisen und daher spezielle elektronische Eigenschaften versprechen. Die experimentellen HRTEM Aufnahmen zeigen die wohldefinierte, atomare Struktur der CSL Korngrenzen im Vergleich zu anderen.

1. Introduction

Using ceramic materials, special electronic devices, like transistors, will become more stable and can operate at higher temperatures. These electronic devices require a special bicrystal with well-defined atomic structure in order to perform a certain structure of the electronic density of state. At zinc oxide varistors [1 to 9] the double Schottky barrier at grain boundaries has been studied already in detail and simulations of the electronic behavior already show the important influence of the grain boundary thickness [1]. In order to understand this behavior, HRTEM investigations have been carried out to detect the crystalline structure of grain boundaries [2, 4 to 6]. The grain boundaries usually have lower density of atoms than the bulk specimen, so this device finally possesses a more narrow band gap than the single crystal. Also alumina with its high temperature resistance has already been studied for this purpose [10]. The bonding lengths among grain boundary atoms were found to be different than in bulk material. Examples for the successful use of special grain boundaries are the weak links in

[1]) Now at: Nagoya Institute of Technology, Materials Science Department, Gokisocho, Showa-ku, 466-8555 Nagoya, Japan.

some superconductor devices and examples for the open structures at grain boundary have been found especially in materials with large unit cells like spinell or perovskite structure.

For the classification of special grain boundaries several geometrical models have been developed, the most famous one is the coincidence site lattice (CSL) theory [11 to 14], but also the coincidence of reciprocal lattice planes (CRLP) [15 to 17] and the *d*-spacing-concept [13, 14, 18] are well established and are described in detail later. The latter one is called in this paper the model of low index lattice planes of supercells (LIPS). Among all grain boundaries in polycrystalline materials special boundaries can be classified by a low value of Σ, which describes the density of coincidence points according to the CSL theory. These special boundaries have other properties than random boundaries, particular the grain boundary energy is generally lower. The structural unit model [13, 14, 19] was able to show that these grain boundaries consist of special atomic configurations in the grain boundary core which are significantly different compared to the coordination of atoms in the single crystal. The structural units are found to be stable over a wide temperature range. The structural unit model has successfully been used for the description of the atomic structure of grain boundaries not only in metals.

Zinc oxide possesses wurtzite-type structure which consists of the hexagonal lattice with a *c/a* ratio of 1.602. Aluminum nitride has the same structure and nearly the same *c/a* ratio, so all results of this paper concerning the geometrical relationship of grain boundaries are valid for both materials. Also the *c/a* ratios of other materials with wurtzite-type structure are close to this value, such as for InN, MnS and one modification of TaN, while, however, for gallium nitride the *c/a* ratio (1.622) deviates too much.

The aim of this paper is to describe the successful search for special grain boundaries in ZnO and AlN by using three different geometrical models. The atomic structure of the most promising ZnO grain boundaries was calculated by molecular dynamics simulations and the structural units are analyzed. The experimental observations with high resolution transmission electron microscopy (HRTEM) described in the following section support these results and are finally discussed by comparing them to other results.

2. Methods

2.1 Coincidence site lattice (CSL)

The basic idea of the coincidence site lattice theory [13] is that special grain boundaries are defined by assuming a hypothetical three-dimensional interpenetrating of both lattices, at which one part of the atoms ($1/\Sigma$) are sitting on coincidence positions which belong to atomic positions in both grains. The lower the Σ value, the more atoms are sitting on coincidence sites belonging to atomic positions of both lattices. Thereafter the grain boundary plane is defined, which means that the definition of the Σ value is independent of the choice of this plane.

The Σ value was calculated by geometrical analysis of the coincidence in plots of the atomic structure. The search was focussed on symmetrical tilt grain boundaries (STGB) where the two facing grains possess the same zone axes, but are rotated to each other around this axis by the angle of misorientation Θ as shown in Fig. 1.

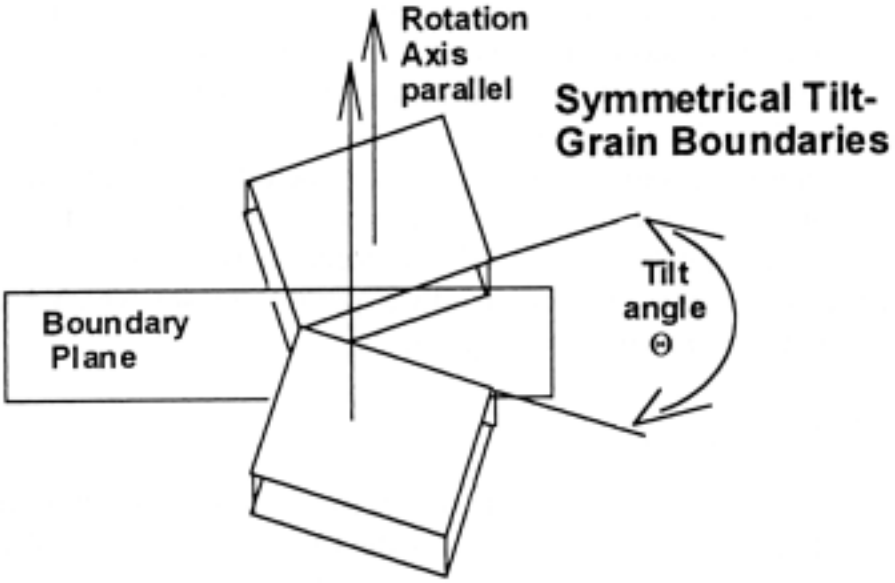

Fig. 1. Definition of the angle of misorientation Θ for symmetrical tilt grain boundaries

2.2 Coincidence of reciprocal lattice points (CRLP)

The coincidence of lattice points in reciprocal space [15 to 17] is worthwhile to be considered, because each lattice point in the reciprocal space represents a set of parallel planes in real space, as seen in a TEM diffraction pattern. Hence, the coincidence of reciprocal lattice points of two lattices means a perfect matching of real space lattice planes. In order to find these coincidences, the total sum of overlap of the reciprocal lattice points is calculated and summed up by a computer program [16]. The algorithm used in this program treats the reciprocal lattice points as spheres with a certain radius and their sum of overlap is plotted as a function of the misorientation angle, as explained in detail elsewhere [16]. By varying the size of this radius also grain boundaries with near coincidence [10, 20] can be found (indicated in this paper with Σ in parentheses), which means, a close degree of parallelness and similarity in interplanar spacing. The calculation is applicable for any homophase or heterophase interface very easily and the results are consistent with experimental observations for a variety of materials [16, 17].

2.3 Low index plane supercell (LIPS)

The idea to consider the low index planes of supercells (LIPS) [14, 18] of grain boundaries arose by comparing interfaces with crystal surfaces. If low index planes lie parallel to the boundary plane, they have a larger lattice spacing, the so called d-spacing. The atomic density in these low index planes is higher than in other planes and hence, these boundaries should have special atomic arrangements, and properties as well. This model is also known as the d-value model. The search was performed by using the stereographic projections and commercial computer programs for crystallography. For the chosen zone axis the low index planes were searched for and then their corresponding angles of rotation $\Theta/2$ were calculated.

2.4 Molecular dynamics

After the above described geometrical analysis the atomic structure of these grain boundaries is calculated by the molecular dynamics method. The upper half of the MD

supercell was determined by rotating the unit cell and the lower half is formed by a 180° mirror operation. The supercell was chosen to have at least a size of about $10 \times 3 \times 1$ nm^3 with about 4000 atoms, in order to avoid any interaction effects between the two grain boundaries which are formed by using the periodic boundary conditions. The MD calculations were performed by using the program "Moldy" which includes the long range Coulomb interaction by performing the Ewald sum in reciprocal space. This code has been tested for several material science problems [22, 23]. The forces between Zn–O and O–O atoms are calculated by the Buckingham potential with a parameter set which has been successfully used for calculations on zinc oxide [3, 9, 21]:

$$E_R = \frac{z_i z_j e^2}{r} + A \exp\left(\frac{-r}{B}\right) - \frac{C}{r^6} .$$

The parameters were $A = 529.7$ eV, $B = 0.03581$ nm, $C = 0$ for the Zn^{2+}–O^{2-} bonding, and $A = 9547.96$ eV, $B = 0.021916$ nm, $C = 32 \times 10^{-6}$ nm for the O^{-2}–O^{-2} bonding. The calculations were performed in the N, p, T ensemble at constant atmospheric pressure. By several trials the following sequence for the temperature schedule was determined in order to find the energy minimum of the system: 4000 time steps at 950 K, then slow cooling in five steps to 300 K and again running 2000 time steps. Temperatures higher than 1000 K were found to cause a large disordering within the grain boundary region and were avoided.

3. Results

3.1 Geometrical analysis

The geometrical analysis was focussed on symmetrical tilt grain boundaries with a certain angle of misorientation Θ, as defined in Fig. 1. Using the CRLP model the sum of the coincidence lattice planes $h(\Theta)$ is plotted in Fig. 2 as a function of the misorientation angle for the three zone axes [0001], [10$\bar{1}$0] and [11$\bar{2}$0] in the four-point notation and [001], [1$\bar{1}$0] and [1$\bar{2}$0] in the three-point notation, in the following called *c*-, *a*-, *b*-axes. This sum represents the intensity of the coincidence and shows several peaks at angles where grain boundaries with a large amount of coincidence sites occur. The heights of these peaks are proportional to the amount of coincidence and are indicated in Table 1 with the letters vw for very weak, w weak, m middle, s strong, ss super strong. The values of the corresponding angles give the orientation relationship for the grain boundaries with high coincidence.

In order to check this analysis, the two other models were also applied and the comparison of the results of the three methods, the CSL, CRLP and LIPS model, is shown in Table 1. The angle of misorientation Θ is printed in the first column of this table and in the second column the exact Σ values (or the near Σ values in parentheses) are printed. The third column displays the results of the CRLP-model calculations, which were taken from the plot in Fig. 2. The corresponding angles Θ which are in most cases the same as for the other models are printed in this column of the table. Finally in the last column the result of the LIPS model is presented: The normal directions [*uvw*] of low index planes parallel to a STGB-grain boundary were searched for and are displayed in three-point notation. These directions are identical to the 180° rotation axis in the CSL model. Another criterion used for this analysis is the final size of the resulting supercell. Thereafter, for each of them their misorientation angle was calculated and inserted in the corresponding row of the table.

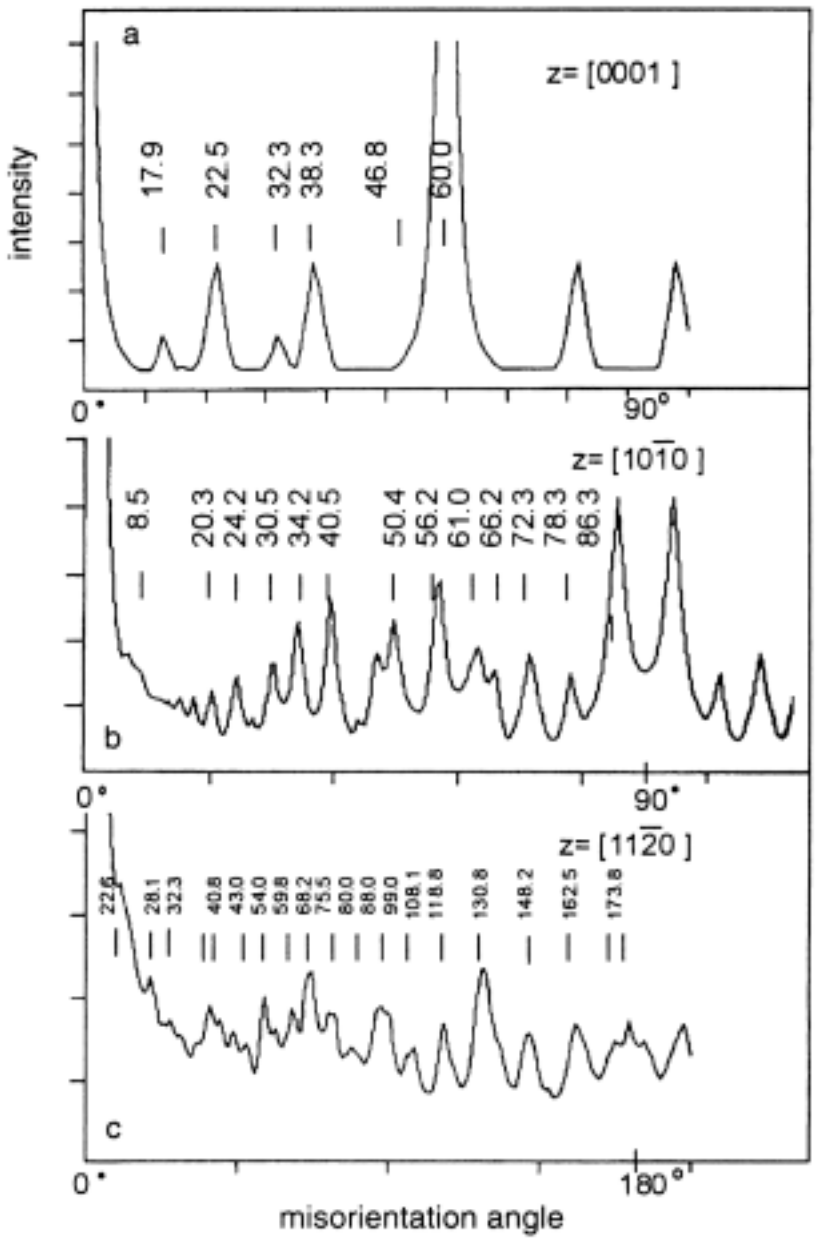

Fig. 2. Intensity of the coincidence of reciprocal lattice points (CRLP) as a function of the misorientation angle of ZnO and AlN symmetrical tilt grain boundaries for the three zone axes a) [0001], b) [10$\bar{1}$0], c) [11$\bar{2}$0]

The three methods show mostly identical results, as can be seen by the good agreement in the angles for grain boundaries detected by the exact geometric CSL and LIPS models (column 1) compared to those found by the (numerical) CRPL model (column 3). For the grain boundaries with *c*-axis orientation the coincidence is the same for all hexagonal lattices no matter which *c*/*a* ratio they possess [12]. For the *c*-axis orientation, due to the sixfold symmetry, there are two different ways to describe the crystallographic direction of any plane containing this *c*-axis. For this zone axis the computer program using the CRLP model cannot predict all special grain boundaries and also the angle sometimes deviates of more than 1 compared to the other models, which has to be considered in a further version of this program. For the *a*- and *b*-axes all three models showed several special grain boundaries in good agreement. The CSL model [12] describes two cases of exact coincidence, $\Sigma = 13$ and $\Sigma = 17$, but also all other cases of near coincidence found independently with the two other models are of physical relevance and have to be considered. The peaks indicating the coincidence are rather weak and sometimes disappear if the size of the reciprocal lattice points is changed, indicating that the coincidence of these boundaries is not so sharp. The cases were

Table 1
List of symmetrical tilt boundaries for three different zone axes detected by three different methods and comparison of the calculated angles

misorientation angle Θ	CSL model Σ values	CRLP model Θ, peak int.	LIPS model cell planes
z = [0 0 1]			
17.9°	31	–	[7 $\bar{4}$ 0] or [5 $\bar{1}$ 0]
21.8°	21	22.5° m	[1 $\bar{2}$ 0] or [4 $\bar{1}$ 0]
27.8°	13	32.3° w	[3 $\bar{1}$ 0] or [2 $\bar{5}$ 0]
38.2°	7	38.3° m	[2 $\bar{1}$ 0] or [1 $\bar{4}$ 0]
46.8°	19	–	[1 $\bar{7}$ 0] or [2 $\bar{3}$ 0]
60.0°	3	60.0° ss	[1 $\bar{1}$ 0] or [2 $\bar{1}$ 0]
z = [1 $\bar{1}$ 0]			
10.4°	(49)	8.5° w	[1 2 $\overline{10}$]
20.4°	(17)	20.3° w	[1 2 $\bar{6}$]
12.2°	(19)	24.2° w	[1 2 $\bar{5}$]
30.1°	(31)	30.5° w	[1 2 $\bar{4}$]
34.2°	(43)	34.2° m	[2 4 $\bar{7}$]
38.7°	(35)	40.5° m	[1 2 $\bar{3}$]
49.6°	(33)	50.4° m	[3 6 $\bar{7}$]
56.8°	(21)	56.2° m	[1 2 $\bar{2}$]
66.2°	(25)	66.2° w	[5 10 $\bar{8}$]
71.6°	(49)	72.3° w	[2 4 $\bar{3}$]
78.4°	(29)	78.3° w	[3 6 $\bar{4}$]
85.6°	(15)	86.3° s	[1 2 $\bar{1}$]
z = [1 $\bar{2}$ 0]			
22.6°	(23)	22.6° w	[1 0 3]
29.8°	13	28.1° w	[6 0 1]
34.6°	(21)	32.3° w	[1 0 2]
40.8°	–	40.8° m	–
43.6°	(59)	43.0° vw	[4 0 1]
56.2°	17	–	[3 0 1]
59.9°	–	59.8° w	–
65.4°	13	68.2° w	[1 0 1]
75.8°	–	75.5° w	–
79.4°	17	80.0° w	[2 0 1]
87.8°	(25)	88.0° vw	[5 0 3]
100.4°	(19)	99.0° w	[4 0 3]
108.8°	–	108.1° w	–
118.8°	–	118.8° w	–
130.8°	(15)	130.8° m	[3 0 4]
148.2°	(73)	148.2° w	[5 0 11]
162.2°	(43)	162.5° w	[1 0 4]
173.8°	–	173.8° vw	–

the size of the supercell was beyond the capability of the computer program are indicated with a vertical bar. The indices of the grain boundary plane sometimes show rather unexpected high values due to the special hexagonal lattice geometry. Each method has its advantages and the combination of all of them gives reliable results. The

results of this geometrical analysis depend only on the lattice symmetry and are therefore valid for all materials with hexagonal crystal structures with a *c/a* ratio of 1.604, especially for ZnO and AlN.

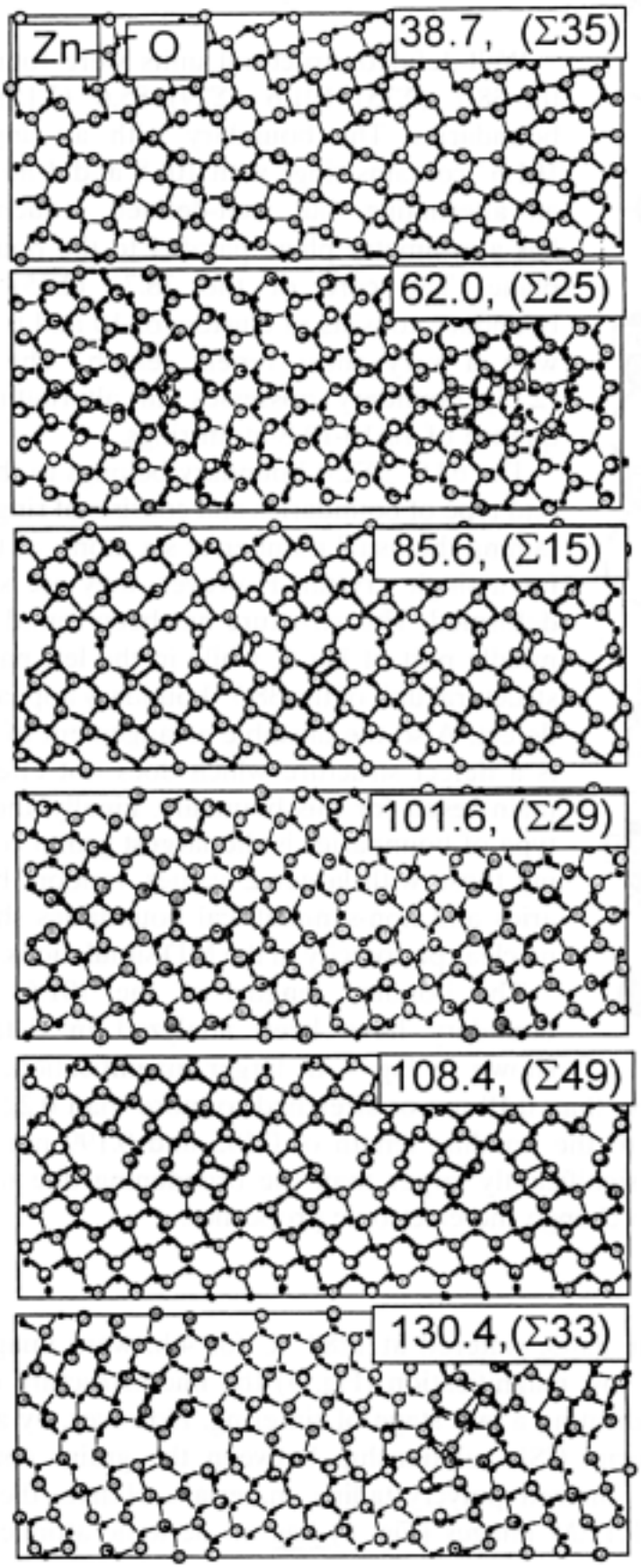

3.2 Molecular dynamics calculation

For the most interesting of these ZnO grain boundaries with the zone axis [1$\bar{1}$0] shown in Fig. 2b the atomic structure was calculated using the MD simulation. The results are shown in Fig. 3 as the average atomic positions at 300 K, where Zn atoms are displayed with a large radius, O atoms with a small radius. The scale of each drawing is $2 \times 5\ nm^2$, but the sizes of the supercells were 6.6×3.0, 9.3×6.4, 16.0×7.2, 13.0×5.4, 14.0×3.8, 9.8×3.6, respectively, in the given order of Fig. 3. The misorientation angle has to be considered up to 180°, because the atomic base has a lower symmetry than the lattice. Three types of atomic structures at the core of grain boundaries in zinc oxide can be defined: 1. Those with well-defined structural units which are significantly different than in the single crystal, 2. those with six-atom rings at the grain boundary core with a similar arrangement as in the single crystal, and finally 3. unstable or undefined atomic structures, indicated in Fig. 3 by mismatches in the atomic columns of the three unit cells perpendicular to the zone axis (e.g. right part of the 62° and the 130.4° grain boundary).

Fig. 3. Atomic structure obtained by molecular dynamics (MD) simulations of some special symmetrical tilt boundaries in ZnO as a function of the tilting angle Θ (in degrees) between the grains

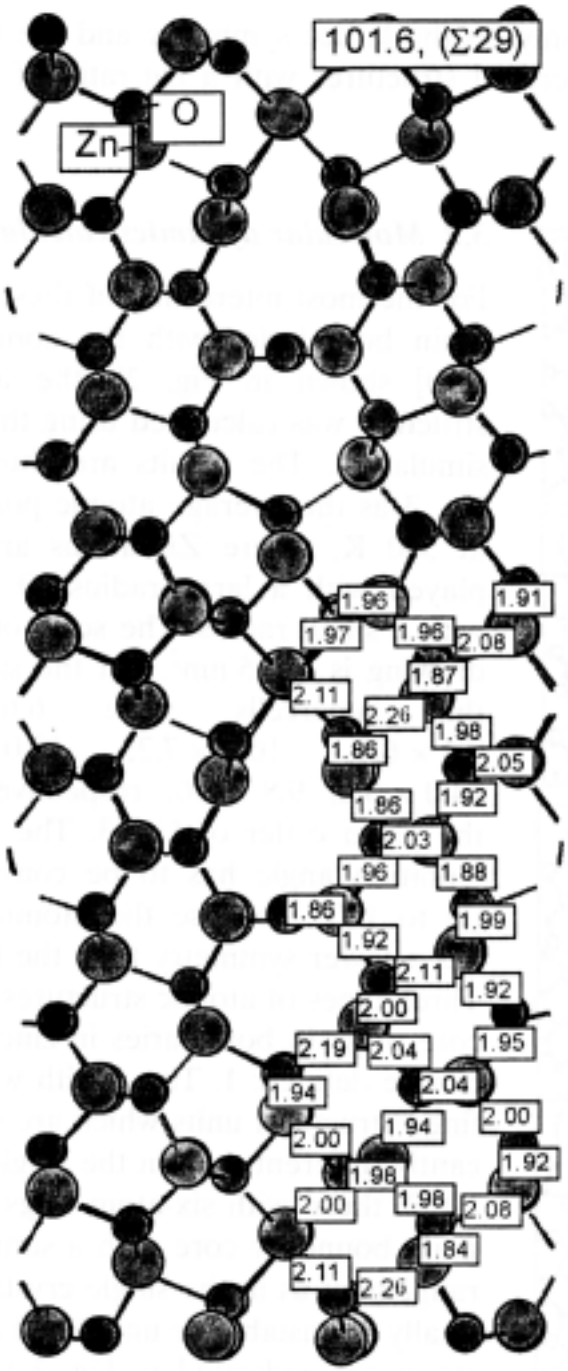

Fig. 4. MD structural model for the core of the 101.6° (Σ29) grain boundary indicating the bonding lengths in units of 0.1 nm (= 1 Å) compared to the bulk structure with 0.195 and 0.199 nm

Well-defined structural units were found for the 38.7° (Σ35), 101.6° (Σ29), 85.6° (Σ15) grain boundaries. The boundary with an angle of 101.6° contains rings with 10, 8 and 4 atoms in an alternating, but well-defined sequence. It has a symmetry plane parallel to the boundary plane. The core of the 38.7° (Σ35) grain boundary consists of clusters of 10 and 6 atoms with a very short repeat length. The 85.6° (Σ15) boundary possesses an alternating sequence of 10-10-10-8-atom rings.

The 62.0° (Σ25) boundary belongs to the second type of boundaries and consists of rings containing the usual number of six atoms as typical for a single crystal. However, they are slightly deformed. This structure has been found in the middle part of Fig. 3, while in the left part one structural unit of the 38.7° boundary appears as a defect. Also the unstable arrangement of atoms is a defect structure which does not effect the main result for this boundary. Finally, the third type of boundaries is the largest group containing those with larger Σ values, random boundaries and non-symmetrical boundaries showing no clear periodicity in the MD simulations.

The bonding lengths of the 101.6° (Σ29) boundary have been analyzed in detail, as shown in Fig. 4 in larger magnification. Some Zn–O bonds are compressed to less than 0.18 nm or stretched to more than 0.22 nm at the edges of the rings, compared to the bonding length of 0.195 and 0.199 nm in the single crystal. The deviations are significantly larger than the broadening due to thermal vibrations and are supposed to change the electronic properties.

3.3 Experimental results

Grain boundaries in polycrystalline ZnO, sintered at 1280 °C for 4 h, were imaged by HRTEM using a Topcon 002B. In low magnification (Fig. 5) the microstructure clearly shows straight grain boundaries indicating a late stage of sintering. However, by analyzing the diffraction pattern no special CSL relationship between the grains could be found, as frequently observed in sintered polycrystalline materials. Hence, the grain boundary core as found in the HRTEM images (Fig. 6) has no periodic atomic struc-

Fig. 5. TEM micrograph of sintered (1280 °C, 4 h) ZnO microstructure

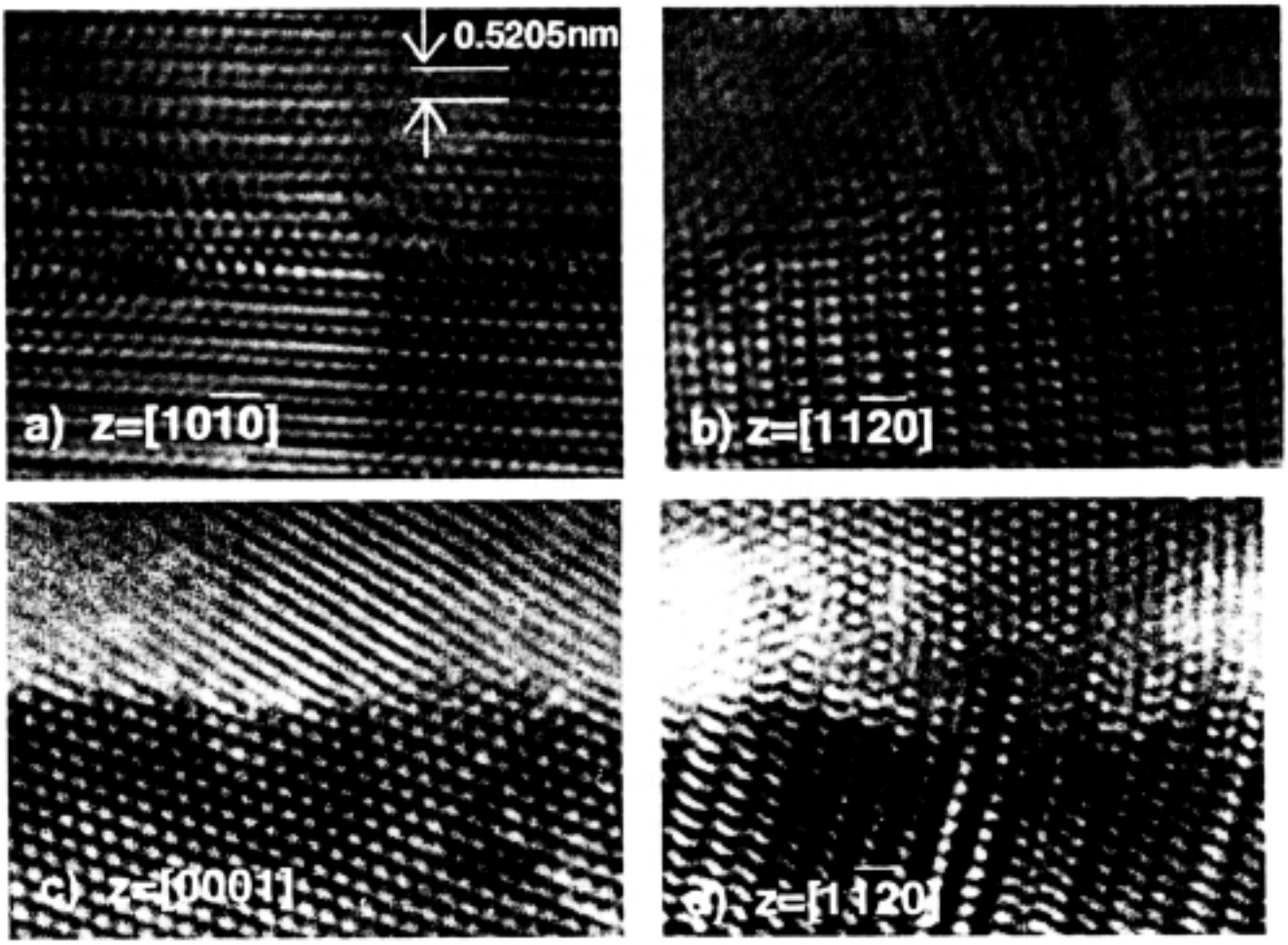

Fig. 6. HRTEM micrographs of random grain boundaries in polycrystalline ZnO imaged with different zone axes, showing crystalline grain boundary structure

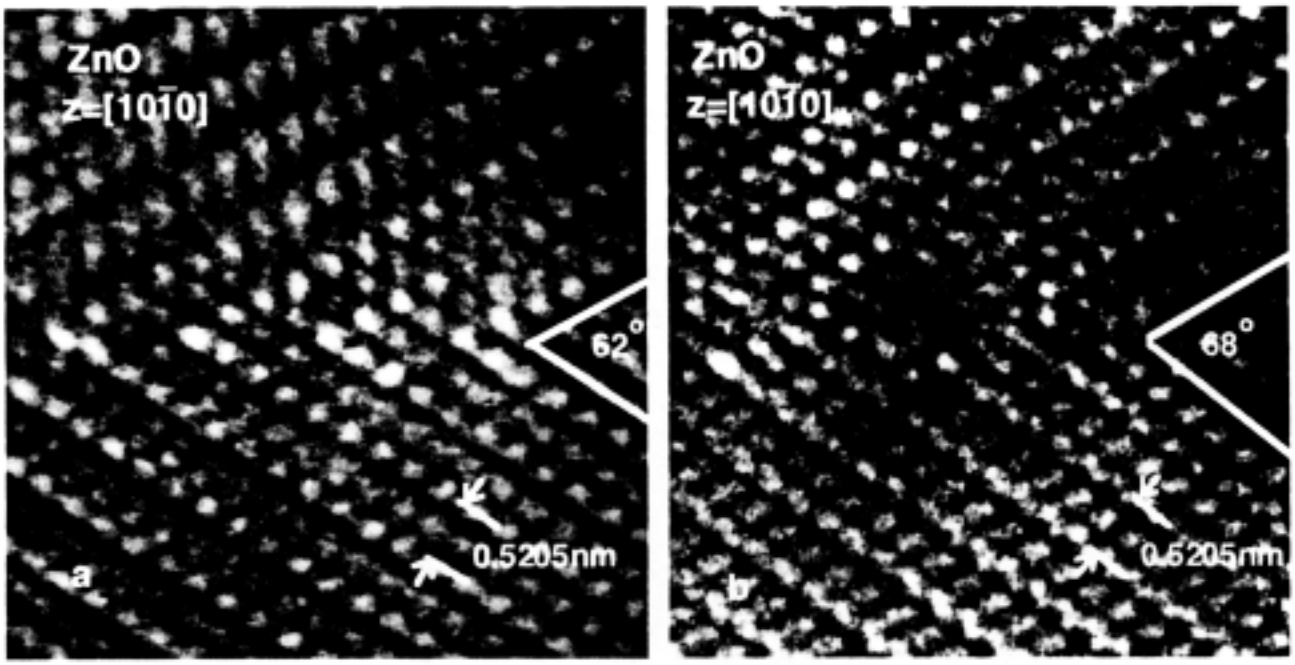

Fig. 7. HRTEM micrographs show the difference of a) a special grain boundary (62°) compared to b) a random boundary (68°, without any special coincidence)

ture. All these grain boundaries were crystalline and not amorphous, indicating the stability of the wurtzite structure even in the grain boundary core.

However, special grain boundaries were found in an internal oxidized Pd–Zn alloy [24]. Within the Pd matrix ZnO precipitates are formed with a size of 100 nm. These precipitates contain symmetrical tilt grain boundaries in *a*-axis orientation, which were imaged by HRTEM using a JEOL 200CX with a point-to-point resolution of 0.20 nm operated at 200 kV. The analysis of the HRTEM micrographs shows that the angle of these grain boundaries changes according to the growth mechanism and the minimum of phase energy [25]. The boundaries with an angle of 62° according to the special CSL orientation relationship of near-$\Sigma 25$ have a well-defined structure: The contrast of the lattice planes in Fig. 7a clearly indicates the well-defined atomic positions with periodicity in the contrast. Hence, the atomic structure consists of stable structural units. For a grain boundary, however, where the tilting angle is increased only a few degrees to the value of 68°, the coincidence is lost and a non-periodic structure is formed. The HRTEM micrograph of this boundary (Fig. 7b) has a dark, unclear contrast, indicating strain fields due to irregular, not well-defined atomic positions.

4. Discussion

The experimental HRTEM micrographs are the evidence, that for zinc oxide, as for many other materials the same rule is observed: The CSL boundaries have really a special atomic arrangement compared to the other randomly oriented ones and the well-defined structural units with their ordered atomic positions with low periodicity are unique for those special tilting angles where the coincidence rule is fulfilled properly. The geometrical analysis leads to special grain boundaries with rather high Σ values compared to metals, which can be explained by the lower symmetry of the wurtzite structure.

The MD calculations for the experimentally observed 62° (Σ25) boundary (Fig. 7a) showed the presence of structural units. The same boundary was observed by HRTEM and in this image also structural units are present indicated by the periodic contrast. However, at the boundary with an angle of 68°, which means a boundary out of low coincidence, those units were omitted indicated by the non-periodic contrast. Quantitative image calculations in order to determine the atomic positions exactly should be performed in future to prove the agreement between calculated and observed structural units. Each structural unit at the grain boundary consists on atomic scale in three variants, whether the ZnO tetrahedera are facing at the boundary plane tip-to-tip or bottom-to-bottom or tip–bottom. This arrangement of the tetrahedera will lead to a positively charged boundary, a negatively charged or a non-polar boundary, similar as calculated for SiC [26] with zincblende structure. With the recent progress in quantitative HRTEM contrast analysis it should be possible to distinguish these variants experimentally.

The molecular dynamics calculations presented in this work were able to find ZnO grain boundaries with stable structural units. Rings with 6 atoms have a similar morphology with those of the bulk crystal, they certainly have the lowest energy. Rings containing a smaller number of atoms than the single crystal rings (4) have a larger energy, because there the atomic coordination is changed drastically. On the other hand, at the 10-atomic ring the bonding lengths (Fig. 4) are in average smaller than in the single crystal, which will lead to a larger energy due to the asymmetry in the potential. Both effects are obviously contrary and are worthwhile to be studied in detail. The structural unit model successfully applied for metals could explain the well-defined sequences of structural units, which will change systematically by increasing the angle of misorientation. In order to prove the whole range of misorientation angles for ZnO grain boundaries, more effort has to be done, since it cannot be excluded that there might exist other grain boundaries with stable structural units.

In zinc oxide the part of covalent bonding is rather high, which supports the short-range structural elements like atomic rings or clusters. The extreme would be an amorphous structure with only short-range order as observed when the quartz structure of SiO_2 is rapidly quenched to glass material. These amorphous structures, however, are not observed in ZnO, even at random tilt- or undefined grain boundaries as observed by the HRTEM micrographs in Fig. 5. Hence, also other forces must act: The ionic bonding forces between the Zn^{2+}- and O^{2-} ions have rather large, long-range interactions. This is the reason, why the coincidence concept works well for ceramics with high amount of ionic bonding, like CdO or MgO [13]: The purely geometrical concept of the coincidence model makes sense not only for metals where each lattice point represents an atom, but also for ceramics, where the unit cell contains more than one atom and, hence, the lattice points are not directly related any more to atomic positions. These long range Coulomb interactions are the physical principle, why the CSL theory works with great success also for ceramics.

Aluminum nitride has the same crystal structure and nearly the same *c/a* ratio as zinc oxide, so the results of the geometrical analysis are the same as for ZnO. But it is known, that nitrides generally have a higher amount of covalent bonding and especially the bonding angles are more stiffer in these materials. MD calculations using the three-body potential with the Born-Mayer-Higgs-type [27] have been successfully used for simulating the thermal conductivity of AlN single crystals. Concerning the grain boundary, the structural units predicted for ZnO could be even more stable in AlN.

The atomic structural units for ZnO grain boundaries show open structures with rings of atoms with a larger number of atoms than in the single crystal. This excess volume allows electrons of the conduction band to be trapped in this energetically favorable places, because they are repulsed from the deep potential of the valence electrons into the empty space at the grain boundary core. Hence, the electronic band gap of grain boundary atoms will be smaller as shown in a previous works on alumina [10]. It is the goal of further engineering on atomic scale to influence this gap and the barrier height at grain boundaries more precisely for practical applications by taking the advantage of the results published in this paper. The next step after experimental verification will be electronic band structure calculations, so that the goal, producing a ceramic transistor with higher temperature performance, will be reached in near future.

5. Conclusion

The geometrical analysis using three different models gives for the first time a complete list of the most interesting symmetrical tilt grain boundaries with wurtzite-type structure and is valid for ZnO and AlN. At special ZnO grain boundaries atomic structural units have been found which are stable after long-time MD simulations. The units consist of rings with 10 or 8 atoms, more than in the single crystal and have a large excess volume. The bonding lengths between atoms for the most promising candidate for varistor applications have been characterized. The experimental HRTEM micrographs show indeed the occurrence of structural units for the coincidence boundary and non-periodic contrast for the non-coincidence boundary.

Acknowledgements The idea of this work was introduced by Prof. Yuichi Ikuhara. Fig. 6 was provided by Takashi Ichimori. The specimens were received from Masatada Yodogawa. Dr. Craig Fisher helped concerning the "Moldy" program very much. The financial support came from the NEDO project "frontier ceramics" under the leadership of Dr. N. Shibata.

References

[1] C.W. NAN and D.R. CLARKE, J. Amer. Ceram. Soc. **79**, 3185 (1996).
[2] H.T. SUN, L.Y. LING, and X. YAO, J. Amer. Ceram. Soc. **76**, 1150 (1993).
[3] D.J. BINKS and R.W. GRIMES, J. Amer. Ceram. Soc. **76**, 2370 (1993).
[4] H. CERVA and W. RUSSWURM, J. Amer. Ceram. Soc. **71**, 522 (1988).
[5] J.C. KIM and E. GOO, J. Amer. Ceram. Soc. **73**, 877 (1990).
[6] W. WUNDERLICH, Proc. 6th Internat. Symp. Ceramic Materials for Engines, Arita, Oct. 1997, Ed. K. NIIHARA et al., Technoplaza Co. Ltd., ISBN 4-9980630-0-6, 1998 (p. 540).
[7] M.A. MCCOY, R.W. GRIMES, and W.E. LEE, J. Mater. Res. **11**, 2009 (1996).
[8] M.A. MCCOY, R.W. GRIMES, and W.E. LEE, in: Proc. Conf. Electroceramics, Vol. 2, Eds. J.L. BAPISTA, J.A. LABRINCHA, and P.M. VILARINHO, Aveiro (Portugal), 1996 (p. 549).
[9] R.W. GRIMES, D.J. BINKS, and A.B. LIDIARD, Phil. Mag. **A72**, 651 (1995).
[10] S.D. MO, W.Y. CHING, and R.H. FRENCH, J. Amer. Ceram. Soc. **79**, 627 (1996).
[11] H. GRIMMER, B. BONNET, S. LARTIGUE, and L. PRIESTER, Acta. Cryst. **A40**, 108 (1984).
[12] H. GRIMMER, ACTA CRYST. **A45**, 320 (1989).
[13] A.P. SUTTON and R.W. BALLUFFI, Interfaces in Crystalline Materials, Clarendon Press, Oxford 1995.
[14] D. WOLF and S. YIP, Material Interfaces, Chapman & Hall, London 1992.
[15] N.H. FLETCHER and P.L. ADAMSON, Phil. Mag. **14**, 99 (1966).
[16] Y. IKUHARA and P. PIROUZ, Mater. Sci. Forum **207**, 121 (1996).

[17] S. Stemmer, P. Pirouz, and Y. Ikuhara, Phys. Rev. Lett. **77**, 1797 (1996).
[18] A.P. Sutton, Progr. Mater. Sci. **36**, 167 (1992).
[19] A.P. Sutton and V. Vitek, Phil. Trans. Roy. Soc. **A309**, 1 (1983).
[20] T. Hoeche, P.R. Kenway, M. Rühle, H.-J. Kleebe, and P.A. Morris, J. Amer. Ceram. Soc. **77**, 339 (1994).
[21] G.V. Levis and C.R.A. Catlow, J. Phys. C **18**, 1149 (1985).
[22] K. Refson, Physica **131B**, 256 (1985).
[23] K. Refson and G.S. Pawley, Mol. Phys. **61**, 669 (1987).
[24] T. Ichimori, T. Katoh, H. Ichinose, K. Ito, and Y. Ishida, Interface Science and Mater. Intercon. Proc. Conf. JIMIS-8, Jpn. Inst. Metals, 1996 (p. 359).
[25] P. Nikolopoulos, J. Mater. Sci. **20**, 3993 (1985).
[26] M. Kohyama and R. Yamamoto, Phys. Rev. B. **49**, 17102 (1994); **50**, 8502 (1994).
[27] H. Kitagawa, Y. Shibutani, and S. Ogata, Model. Simul. Mater. Sci. Engng. **3**, **21** (1995).